Chem. Eng. Comm., 190: 1267–1292, 2003

ISSN: 0098-6445 print/1563-5201 online
DOI: 10.1080/00986440390215388

Taylor & Francis
Taylor & Francis Group

ATOMISTIC MOLECULAR DYNAMICS SIMULATIONS OF GAS DIFFUSION AND SOLUBILITY IN RUBBERY AMORPHOUS HYDROCARBON POLYMERS

SABRINA PRICL
MAURIZIO FERMEGLIA

Computer-Aided Systems Laboratory,
Department of Chemical, Environmental and
Raw Materials Engineering, University of Trieste, Trieste, Italy

Diffusion coefficients D of H_2, He, O_2, N_2, and CO_2 in different rubbery amorphous polymeric matrices were estimated by atomistic molecular dynamics simulations at 298 K using the Einstein relationship, and compared with the relevant experimental values, where available. The simulated diffusion coefficients D of all the gases in all polymers considered almost regularly decreased with increasing molecular gas volumes and increasing polymer glass transition temperature. Further, solubility coefficients and heats of solution were obtained for all gases from Grand Canonical Monte Carlo simulations, which were also used to calculate sorption isotherms. In general, there is a good agreement between experimental and simulated values of diffusion and solubility coefficients for all gases considered.

Keywords: Molecular quantum mechanics; Molecular dynamics simulations; Rubbery amorphous polymers; Diffusion coefficient; Solubility

Received 9 February 2001; in final form 19 August 2001.

Address correspondence to Sabrina Pricl, Computer-Aided Systems Laboratory, Department of Chemical, Environmental and Raw Materials Engineering, University of Trieste, Piazzale Europa 1, 34127 Trieste, Italy. Fax: 39 040.569823. E-mail: sabrina@dicamp.univ.trieste.it

INTRODUCTION

Gas diffusion phenomena in polymeric systems are of topical importance for a number of practical applications, ranging from selective gas separation through membranes and formulation of new food packaging materials to the design of novel pharmaceutical systems for controlled drug delivery. Under common circumstances, the process of gas permeation in polymeric matrices can be satisfactorily described, at the macroscopic level, by solving the classical Fick's law of diffusion (Crank and Park, 1968; Crank 1975; Stern and Trohalaki, 1990). On a microscopic scale, however, the picture of the mechanism of gas diffusion in chain systems is still rather unfocused, and the available literature descriptions lay their foundations mainly on phenomenological bases (Stern and Trohalaki, 1990; Petropoulos, 1970; Koros and Paul, 1978; Kulkarni and Stern, 1983; Stern et al., 1986; Zhou and Stern, 1989). This poses a notable limitation, since the parameters of any phenomenological model cannot be related to the polymeric structure and, hence, the model cannot be used in a predictive fashion.

In recent years, computer experiments based on molecular mechanics (MM) and molecular dynamics (MD) simulation techniques have marked their breakthrough as new powerful research tools for characterizing the structure and properties of bulk amorphous polymers. The lengths of the trajectories that can be generated on current workstations are of the order of nanoseconds. If this inevitably limits the range of properties that can be studied directly to those that evolve over this time scale, on the other hand it seems to be suitable for the investigation of the diffusion phenomena of small molecular gases within amorphous polymeric matrices. Indeed, it has been experimentally verified that the diffusion coefficients D of the most common gases in several liquid or rubbery macromolecules are such that the average displacement of the diffusant is large enough to be determined within the feasible MD simulation times (Sonnenburg et al., 1990; Takeuchi and Okazaki, 1990; Khrisna Pant and Boyd, 1993; Gusev et al., 1994; Theodorou, 1996; Fried and Goyal, 1998; Charati and Stern, 1998).

The advantages of such virtual experiments are self-evident, for both the determination of the numerical values of D and the possibility of exploring in detail the mechanism of diffusion at the molecular level. Despite this, almost all above-cited investigations are concerned with specific gas/polymer systems, and no detailed study of the effect of a systematic modification in the polymer chemical composition on the diffusion of penetrant gaseous molecules has been performed. Accordingly, the purpose of the present work is to estimate the values of the diffusion coefficients of He, H_2, N_2, O_2, and CO_2 as a function of structural and chemical details for the series of alkane and alkene polymers listed in Table I.

Table 1 Most Common Experimental Values of the Glass Transition Temperature for the Polymers Considered

Polymer	Acronym	T_g^{exp} (K)[a]
Poly(ethylene)	PE	195
Poly(propylene)	PP	263
Poly(isobutylene)	PIB	197
Poly(1,2-butadiene)	1,2PBD	266
cis Poly(1,4-butadiene)	*c*-1,4PBD	159
trans Poly(1,4-butadiene)	*t*-1,4PBD	171
cis Poly(isoprene)	*c*-PIP	203
trans Poly(isoprene)	*t*-PIP	215
cis Poly(chloroprene)	*c*-PClP	253
trans Poly(chloroprene)	*t*-PClP	228

Source: June et al., 1991.

SIMULATION DETAILS

Chain Models

All simulations were performed on a Silicon Graphics Origin 200, using the commercial software Cerius^2 (ver. 4.2) from Molecular Simulation Inc. (for both molecular mechanics (MM) and molecular dynamics (MD) simulations) and in-house developed codes (stand-alone and add-on to the commercial package).

The generation of accurate model amorphous structures of all polymer chains reported on was conducted as follows. For each polymer, the constitutive repeating unit (CRU) was first built and its geometry optimized by energy minimization using the COMPASS force field (Sun and Rigby, 1997; Sun, 1998). The COMPASS FF is an augmented version of the CFF series of force fields (Maple et al., 1988) and is the first ab initio force field that has been parameterized and validated using condensed-phase properties in addition to various ab initio and empirical data for molecules in isolation. The bond terms of the COMPASS FF potential energy function include a quartic polynomial for both bond stretching and angle bending, a three-terms Fourier expansion for torsions, and a Wilson out-of-plane coordinate term. Six cross terms up through third order are present to account for coupling between the intramolecular coordinates. The final two nonbonded terms represent the intermolecular electrostatic energy and the van der Waals interactions, respectively; the latter employs an inverse ninth-power term for the repulsive part rather than the more customary twelfth-power term (see Appendix for details).

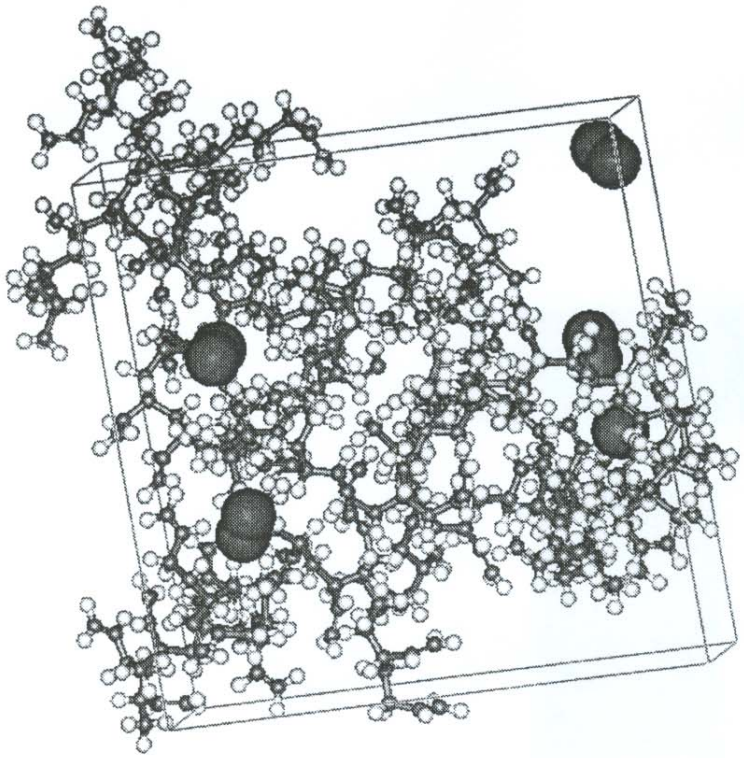

Figure 1. Molecular model of the equilibrated cell containing ten amorphous chains of *trans* poly(1,4-butadiene) and five oxygen molecules at 298 K.

allowed to vary in size and shape during energy minimization, in order to find the equilibrium density for each structure.

Ten independent amorphous structures for each polymer considered in this study were generated according to the procedure described above, and Figure 1 illustrates one of such structures obtained for *trans* poly(1,4-butadiene) as an example. The properties reported below are then to be considered as ensemble averaged from the appropriate set of ten structures.

Model Equilibration

From the fully relaxed models of the corresponding polymeric chains, isothermal-isochoric (*NVT*) MD simulations were run at 298 K to equilibrate the systems, that is, to ensure that their minimized total energy remains constant with respect to the time scale of the simulation used.

The Newton atomic equations of motion were integrated numerically by the Verlet leapfrog algorithm (Verlet, 1967), using an integration step of 1 fs. Temperature was controlled via weak coupling to a temperature bath (Berendsen et al., 1984) with coupling constant $\tau_T = 0.01$ ps. Since the partial charges assigned by the charge equilibration method are dependent on structure geometry, the partial charges were updated regularly every 100 MD steps during the entire MD runs.

Each *NVT* MD equilibration run was started by assigning initial velocity for the atoms according to a Boltzmann distribution at $2 \times T$, and the equilibration process was followed by monitoring the time evolution of the energies. For all polymeric systems considered, the average total, kinetic, and potential energies have ceased to show a systematic drift and have started to oscillate about steady mean values around 50/70 ps. Accordingly, equilibration runs longer than 200 ps (i.e., 200,000 MD steps with time step = 1 fs) were judged not necessary to enhance data accuracy.

Model Validation

The validity of any molecular simulation rests on the suitability and accuracy of the equations used for the intermolecular potentials. Although the accuracy of a prediction may be estimated by considering the approximations and simplifications of the model and computational procedure, the final test lies in a comparison of theoretically predicted and experimentally measured properties. Thus we performed a check of the agreement between simulation and experiment by comparing the simulated *PVT* behavior of the polymer molecules considered with the corresponding available literature data (Rodgers, 1993).

To this purpose, from the fully relaxed models of the corresponding polymeric chains without gas molecules, isothermal-isobaric (*NPT*) MD experiments were run at five different temperatures. Temperature was controlled via weak coupling to a temperature bath (Berendsen et al., 1984) with coupling constant $\tau_T = 0.01$ ps, whereas pressure was kept constant by coupling to a pressure bath (Andersen, 1980), with relaxation time $\tau_P = 0.1$ ps. Again, the partial charges were updated regularly every 100 MD steps during the entire MD runs. Each *NPT* MD run consisted of an equilibration phase of 100 ps during which system equilibration was monitored by recording the instantaneous values of the total, potential, and kinetic energy and the time evolution of the volume, and in a data collection phase, which was extended up to 500 ps.

Another valuable check of the force field and of the operative conditions employed is offered by the cohesive properties, that is the cohesive energy density e_{coh} and the strictly related solubility parameter δ.

In general, e_{coh} is defined as the ratio of the cohesive energy E_{coh} and the molar volume V at a given temperature; E_{coh}, in turn, is defined as the increase in internal energy per mole of substance if all intermolecular forces are eliminated. In our simulated systems, other chains that are simply displaced images of the chain themselves surround the polymer chains. The cohesive energy is the energy of interactions between these images. Accordingly, the values of E_{coh} at different temperatures can be obtained from simulation by calculating the difference between the nonbonded energy of the periodic structure $E_{nb}^{periodic}$ and the corresponding value for an isolated parent chain in vacuum $E_{nb}^{isolated}$:

$$E_{coh} = E_{nb}^{isolated} - E_{nb}^{periodic}. \tag{1}$$

To this purpose, ten parent chains for each polymer were generated and their energy minimized according to the procedure described in the simulation details section. The simulated annealing method was again applied as described above to these systems to provide thermal energies to cross energy barriers between conformation local minima. Finally, NVT MD simulations were performed on the single chains (again the ten best relaxed chains for each polymer) in vacuum at the same temperature conditions applied to the simulations of the relevant periodic systems.

Determination of the Diffusion Coefficient

When mass, energy, or momentum is transferred through a system, the transport is described, to first order, by a phenomenological relation of the general form Flux = -coefficient × gradient. We normally think of these laws applied to nonequilibrium situations but, in addition to these conditions, the linear transport equations also apply to microscopic fluctuations that occur in a system at equilibrium. Thus, the transport coefficients, which are properties of matter, can be extracted from equilibrium molecular dynamics simulations.

To illustrate this in the particular case of gas transport in the equilibrate microstructures of the polymers studied, consider one-dimensional diffusion as described by Fick's law:

$$N\dot{x} = -D\frac{\partial N}{\partial x}, \tag{2}$$

where $N = N(x, t)$ is the number of atoms per unit volume located at position x at time t, $\dot{x}$ is the local velocity at (x, t), and D is the diffusion

coefficient. Then, $(N\dot{x})$ is the flux. From a material balance on a differential element of fluid, we obtain the equation of continuity for mass:

$$\frac{\partial N}{\partial t} + \frac{\partial (N\dot{x})}{\partial x} = 0, \tag{3}$$

and combining these two equations gives the diffusion equation:

$$\frac{\partial N}{\partial t} = D\frac{\partial^2 N}{\partial x^2}. \tag{4}$$

For a set of initial conditions, the diffusion equation can be solved for the temporal and spatial evolution of $N(x, t)$. For instance, if N_0 atoms were concentrated at the origin $x = 0$ at time $t = 0$, then the solution to Equation (4) is given by:

$$N(x, t) = \frac{N_0}{2\sqrt{\pi D t}} \exp\left[\frac{-x^2}{4Dt}\right]. \tag{5}$$

Thus, at any time $t > 0$, the atoms are spatially distributed in a Gaussian about the origin, and as time evolves, atoms diffuse away from the origin, causing the Gaussian to collapse. At any time $t > 0$, the second moment of the distribution gives the mean-square displacement of atoms:

$$\left\langle [x(t) - x(0)]^2 \right\rangle = \frac{1}{N_0} \int x^2 N(x, t) dx. \tag{6}$$

Placing Equation (5) into Equation (6) and performing the integration, we find that the mean-square displacement is simply related to the diffusion coefficient:

$$\left\langle [x(t) - x(0)]^2 \right\rangle = 2Dt. \tag{7}$$

This result applies when the time t is large compared to the average time between collisions of atoms. The three-dimensional analog of Equation (7) is:

$$\lim_{t \to \infty} \frac{\left\langle [r(t) - r(0)]^2 \right\rangle}{6t} = D. \tag{8}$$

In realizing Equations (7) and (8) from simulation, the brackets would be interpreted as averages over time origins. Since at a specified state condition the diffusion coefficient is a constant, Equation (8) implies that the mean-square displacement grows linearly at large delay times. Equation (7), originally derived by Einstein, belongs to the family of fluctuation-dissipation equations that relate transport properties to time or ensemble averages performed over systems at equilibrium. The validity of such relation rests on the hypothesis that macroscopically prepared gradients are often negligibly small on macroscopic length scales. Therefore, the system response to the macroscopic gradient is fully determined by local (equilibrium) fluctuations, which, in this case, are the random walk motions of the penetrant described by the Einstein expression for the mean-square displacement at equilibrium. Accordingly, relaxation of a macroscopically imposed gradient can be expressed by the same diffusion coefficient we find at equilibrium.

A further consideration is appropriate at this stage. Equation (8) implies that the diffusion coefficient D, being a constant, is independent of the diffusing gas concentration. Indeed, constant D values have been reported for the diffusion of light gases with low critical temperatures in several rubbery polymers. Such gases are only barely soluble in rubbery macromolecules, even at elevated pressures. Accordingly, in our virtual MD experiments for the determination of D we assumed the penetrant gas concentration in the amorphous polymeric matrices to be very low, and this was accounted for by placing only five gas molecules per cubic unit cell.

For the determination of D via virtual experiments, starting from the equilibrated structured obtained by the procedure described above, we performed NVT MD runs at 298 K, during which the mean-square displacements (MSD) $\langle [r(t) - r(0)]^2 \rangle$ of He, H_2, N_2, O_2, and CO_2 were determined from the equilibrated trajectories of the five gas molecules of the same species. The simulation lengths adopted for the estimation of D in the different polymeric matrices are based on the following criteria. According to June et al. (1991), a diffusant molecule must travel a distance at least equal to one unit cell in a microstructure in order to pass from "anomalous" to normal (Einstein) diffusion. Further, the time required by this molecule to travel such a distance increases with an increase in the rigidity of the polymer, that is, with a decrease of its segmental mobility, as reflected by a rise in its glass transition temperature T_g. Therefore, the time necessary for the simulation of normal diffusive motion of a given penetrant molecule in a polymer also must increase with an increase of the polymer T_g.

The most commonly reported literature values of T_g for all the polymers considered (Mark, 1997) are listed in Table I. Accordingly, in the case of those macromolecules having $T_g < 200$ K, a simulation time

of 200 ps was considered sufficient for the diffusant molecules to travel a distance at least equal to one unit cell within this time frame, that is, to obtain a normal diffusive motion of the gases in the relevant amorphous polymeric matrices. For all other polymeric chains, much longer simulation times of at least 1 ns were necessary to obtain the same results.

Calculation of Gas Solubility

Sorption isotherms were obtained by Monte Carlo grand canonical (MCGC) ensemble simulations using the fixed-pressure method of Cerius[2] and some in-house developed routines interfaced to the commercial software. According to the procedure used, the total potential energy E_p of the polymer matrix and the adsorbed molecules is written as the sum of the interaction energy between the adsorbate and the matrix, E_{pAM}, and that between the adsorbates, E_{pAA}. E_{pAM} and E_{pAA} are both written as sums of pairwise additive potentials E_{ij} of the form given by the nonbonded terms of the COMPASS force field (see Appendix). The Lennard-Jones (LJ) potential for the adsorbate-matrix interactions and both the LJ and Coulombic terms for adsorbate-adsorbate interactions were calculated using the minimum image convention (Allen and Tildesley, 1987) with a suitable potential cut off, which was a function of the cell dimensions; no corrections for cutoff were applied in the calculations of gas solubility. The Coulombic term for the adsorbate-matrix interaction was evaluated using the Ewald summation method (Ceperley 1980).

MC simulations in the grand canonical ensemble were carried out using the standard procedure involving creation and destruction of molecules, which interact with the potential field generated by the atoms comprising the polymeric matrix, which is assumed rigid. Molecular creation and destruction attempts are made at points chosen randomly within the matrix (simulation box) with a volume V. In this case, for each polymer a single cell with a density corresponding to the experimental values reported in Table II were used in the calculations. In the GCMC ensemble, the chemical potential μ of the adsorbed molecules equals the chemical potential of the bulk phase, which can be written as a function of temperature T and fugacity f as:

$$\mu = k_B T \ln\left(\frac{f\Lambda^3}{k_B T}\right), \tag{9}$$

in which k_B is Boltzmann's constant and Λ is the thermal de Broglie wavelength. At the low-pressure values considered in this work, bulk gases can be assumed to obey the ideal gas law, and fugacity can be

Table II Comparison Between Experimental and Simulated Cohesive Energy Density e_{coh}, Density ρ, and Solubility Parameter δ Values at 298 K for All the Polymers Considered

Polymer	e_{coh}^{exp} (J/cm^3)[a]	e_{coh}^{sim} (J/cm^3)	ρ_{exp} (g/cm^3)[a]	ρ_{sim} (g/cm^3)	δ_{exp} (MPa$^{1/2}$)[a]	δ_{sim} (MPa$^{1/2}$)
PE	249.2 ÷ 291.8	265.7	0.85	0.86	15.8 ÷ 17.1	16.3
PP	275.6 ÷ 353.4	280.9	0.85 ÷ 0.92	0.86	16.6 ÷ 18.8	16.8
PIB	256.0 ÷ 275.6	257.3	0.84 ÷ 0.93	0.86	16.0 ÷ 16.6	16.1
1,2PBD	–	296.9	0.92	0.96	–	17.2
c-1,4PBD	309.8	313.3	1.01	0.99	17.6	17.7
t-1,4PBD	289.0	304.1	0.93 ÷ 0.97	0.92	17.0	17.4
c-PIP	262.4 ÷ 295.8	285.6	0.900 ÷ 0915	0.89	16.2 ÷ 17.2	16.9
t-PIP	262.4 ÷ 295.8	289.0	0.900 ÷ 0915	0.90	16.2 ÷ 17.2	17.0
c-ClP	282.2 ÷ 368.6	349.7	1.243	1.27	16.8 ÷ 19.2	18.7
t-ClP	282.2 ÷ 353.4	338.6	1.243	1.20	16.8 ÷ 18.8	18.4

[a]Sources: June et al., 1991; van Krevelen, 1990.

replaced by gas pressure, P. This leads to the following expressions for the probability acceptation criteria for molecular creation p_c and destruction p_d, respectively:

$$p_c = \min\left[1, \left(\frac{PV}{(N+1)k_BT}\right)\exp\left(\frac{-\Delta E_p}{k_BT}\right)\right], \tag{10}$$

$$p_d = \min\left[1, \left(\frac{Nk_BT}{PV}\right)\exp\left(\frac{-\Delta E_p}{k_BT}\right)\right], \tag{11}$$

where N is the number of molecules in the simulation box before the molecular movement attempt and ΔE_p is the change in the potential energy associated with the attempts.

In addition to the creation and destruction attempts, which were given equal probability, molecular displacements and rotations were also allowed, each of which was accepted with a probability p given by:

$$p = \min\left[1, \exp\left(\frac{-\Delta E_p}{k_BT}\right)\right]. \tag{12}$$

In the present work, the calculation of ΔE_p was preceded by a check for overlapping interaction sites. If a pair of interaction sites was closer than a preassigned distance, the sites were considered to be overlapping. The distance used for the criterion of overlap was set equal to half the sum of

the van der Waals radii for the two sites. Accordingly, any attempt to create, displace, rotate, or destroy a molecule accompanying an overlapping of sites was discarded. If the sites were not overlapping, ΔE_p was evaluated to determine whether to accept the attempt or not in accordance with the appropriate acceptance probablilities. This procedure amounts to imposing impenetrable hard cores to interaction sites, and therefore the non-Coulombic part of the pairwise interaction potential is the LJ potential supplemented by the hard sphere potential.

Solubility was finally calculated by extrapolating the ratio of the cell loading and the pressure P to zero pressure. As for the MD experiments, also in this case the reported values should be considered as ensemble averaged from the appropriate set of ten structures. A total of 2,500,000 steps was used for each calculation. The molar heat of solution, ΔH_s, was obtained for each gas in each polymeric matrix by studying the temperature dependence of solubility data and applying the well-known Van't Hoff-Arrhenius equation. To this purpose, GCMC simulations were performed at three further temperature values (T = 320, 340, and 360 K, respectively), at a constant pressure of 0.05 bar.

Calculation of the Gas Molecular Volumes

The calculations of molecular volumes were performed using the so-called Connolly dot surfaces algorithm (Connolly, 1983a, 1983b, 1985). Accordingly, a probe sphere of a given radius, representing the solvent molecule, is placed at a tangent to the atoms of the molecule at thousands of different positions. For each position in which the probe does not experience van der Waals overlap with the atoms of the molecule, points lying on the inward-facing surface of the probe sphere become part of the molecule solvent-accessible surface. According to this procedure, the molecular surface generated consists of the van der Waals surface of the atoms that can be touched by a solvent-sized probe sphere (thus called contact surface), connected by a network of concave and saddle surfaces (globally called reentrant surfaces), that smoothes over crevices and pits between the atoms of the molecule. The sum of the contact and the reentrant surface forms the so-called molecular surface (MS); this surface is the boundary of the molecular volume (MV) that the solvent probe is excluded from if it is not to undergo overlaps with the molecule atoms, which therefore is also called solvent-excluded volume. Finally, performing the same procedure by setting the probe sphere radius equal to zero, the algorithm yields the van der Waals surface (WS).

If the Connolly algorithm can be considered a good technique for calculating molecular surfaces, the same procedure has been proved to be less accurate for the determination of molecular volumes. Indeed, it has been observed that the molecular volumes derived using algorithms based

on van der Waals radii are generally 30% lower than the experimentally determined volumes for small molecules (Rellick and Becktel, 1997). Accordingly, for the calculation of the gas molecular volumes, we employed a method based on semiempirical molecular orbital calculations (Fermeglia and Pricl, 1999). First, the electron density distribution of the molecule was determined using the *AM1* algorithm. The software calculates the electron density of the molecule at each point of a grid covering the molecule, allowing the grid size and the space between grid points to be varied. Since the orientation of the molecule within the grid can also be varied, the errors that occur from using a grid of a specific spacing and size can be quantified. The electron density value for each point of the grid was then used to calculate the volume of each molecule as a function of the percentage of the total calculated electronic density, according to a calculation technique proposed by Rellick and Becktel (1997). In this way, no assumption was made about the value of the radii of individual atoms or groups of atoms. Figure 2 is a graphical representation of the molecular volume obtained for CO_2.

RESULTS AND DISCUSSION

Model Validation

All simulated structures were in an amorphous state, as confirmed by inspection of the corresponding radial distribution functions (RDF). At

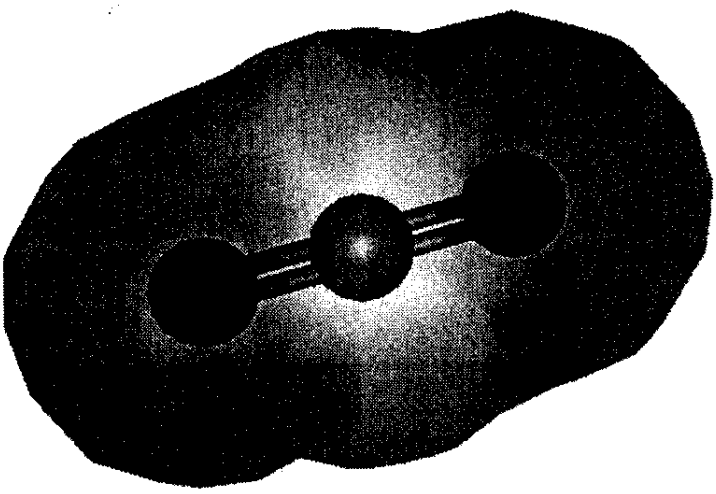

Figure 2. Graphical representation of the molecular volume obtained for CO_2 by the modified Connolly algorithm.

long distances (> 5Å), the RDF for all polymers approach unity, indicating that no long-range structure exists, as one would expect from a purely amorphous system. As stated in the previous paragraphs, the first step in every virtual experiment consists of checking the validity of the generated molecular model and of the relevant expression used for the intermolecular potential. This can be achieved by comparing corresponding sets of experimental and simulated data. Figure 3 is a graphical representation of the results obtained from the comparison between simulated and experimental (Rodgers, 1993) *PVT* behavior for the two macromolecules *cis* poly(1,4-isoprene) and poly(isobutylene), respectively. As appears from this figure, the agreement between real and virtual is rather good, and the same trend has been verified for the entire polymer set examined.

As mentioned in the simulation details section, we performed a further check on data accuracy by calculating the cohesive energy E_{coh} for each polymeric system at 298 K according to the procedure described above. Since the Hildebrand solubility parameter δ (Hildebrand and Scott, 1949) is simply defined as the square root of e_{coh}, we calculated the values of δ at 298 K—using the relevant values of E_{coh} and the density values obtained from the *PVT* simulations—and compared them with the available literature data (June et al., 1991; van Krevelen, 1990). Table II shows that the agreement between the theoretical prediction and experiment is excellent.

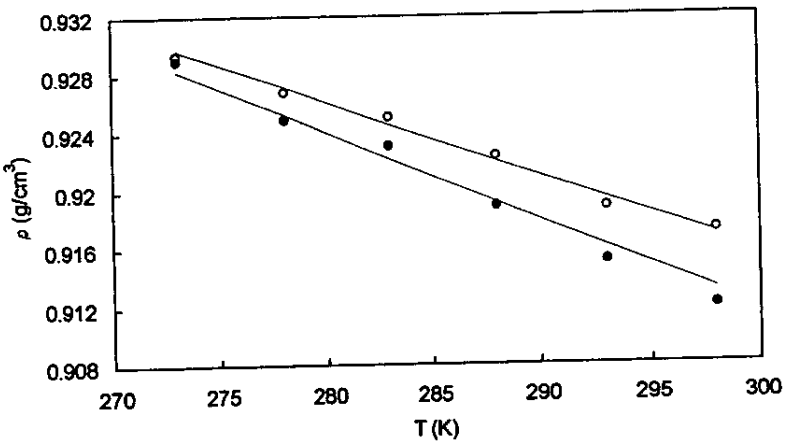

Figure 3. Comparison between experimental (lines) and simulated *PVT* behavior for the two polymers *cis* poly(1,4-isoprene) (filled symbols) and poly(isobutylene) (open symbols).

Diffusion Coefficients

Table III lists the values of the diffusion coefficients D obtained from NVT MD simulations at 298 K for He, H_2, N_2, O_2, and CO_2 in all polymers considered. Table III also shows, for comparison, the experimental values of the diffusion coefficients found in the literature (June et al., 1991; van Krevelen, 1990) for these gases in the corresponding amorphous polymer matrices. As emphasized above, these values are the ensemble average of the appropriate set of 10 structure. If we consider that the accuracy of the estimated values of D is strongly influenced by the density of the polymers, and depends also on the intermolecular potential employed, the duration of the simulation, the cutoff for the nonbonded potential energy components, and other simplifications and assumptions embodied in the MD experiments, from an analysis of Table III we can conclude that the values of the diffusion coefficients D evaluated by simulation are quite satisfactory.

In detail, the estimated vales for He diffusion in all matrices are in excellent agreement with the reported data, being generally about 10% of the corresponding experimental value. In all other cases, the estimated values of H_2, O_2, N_2, and CO_2 in all polymers are about 10–50% of the relevant measured data. In all cases, the magnitude of the simulated gas diffusion coefficients D may be viewed as consistent with the experimental values, if we take into account the assumptions made in the MD simulations, the error intrinsic in any experimental measure, the difference between simulated and experimentally reported polymer densities, and the chain length dependence of D. In fact, a degree of polymerization of 10, such as that used in this work, generally yields diffusion coefficients higher than those obtained with longer chains, due to the larger amount of free volume introduced by chain ends (van der Vegt et al., 1998).

Figure 4 reports, as an example, the mean-square displacements (MSD) of O_2, N_2, and CO_2 in *trans* poly(1,4-butadiene) as a function of time, obtained through the NVT MD simulations. In accordance with Equation (8), the behavior of MSD with time should be linear if the diffusion coefficient D is a constant, that is, for normal diffusion. As can be seen from Figure 4, the relevant plots of MSD vs. t for all gases indeed exhibit linear behavior up to nearly 140–150 ps, whereas the deviation from linearity observed at longer times can be attributed to the increasing statistical error involved in the calculation of MSD.

Another interesting result, which deserves a further comment, is that the values of the simulated diffusion coefficients D of all the gases in all polymers considered almost regularly decrease with the following order: He > H_2 > O_2 > N_2 > CO_2. This coincides with the calculated increasing molecular gas volumes, reported in Table IV. Figure 5 gives a

Table III Comparison Between Experimental and Simulated Diffusion Coefficient Values D (cm^2/s) $\times 10^6$ at 298 K for All the Gases in All Polymeric Matrices Considered

GAS	PE		PP		PIB		1,2 PBD		*c*-1,4 PBD		*t*-1,4 PBD		*c*-PIP		*t*-PIP		*c*-PCIP		*t*-PCIP	
	$D_{sim.}$	$D_{exp.}$[a]	$D_{sim.}$	$D_{exp.}$[a]	$D_{sim.}$	$D_{exp.}$[a]	$D_{sim.}$	$D_{exp.}$[a]	$D_{sim.}$	$D_{exp.}$[a]	$D_{sim.}$	$D_{exp.}$[a]	$D_{sim.}$	$D_{exp.}$[a]	$D_{sim.}$	$D_{exp.}$[a]	$D_{sim.}$	$D_{exp.}$[a]	$D_{sim.}$	$D_{exp.}$[a]
H_2	5.8	–	1.5	–	2.4	1.5	3.4	3.9	20.8	–	13.0	9.6	8.6	10.2	3.4	5.0	2.4	4.3	1.6	–
He	6.9	6.8	1.9	–	6.5	5.9	1.8	2.0	22.9	–	14.8	15.8	20.5	21.4	15.1	–	3.0	5.0	2.1	–
O_2	0.41	0.46	0.18	–	0.057	0.079	0.17	0.14	9.5	–	3.0	1.5	0.98	1.6	0.61	0.70	0.37	0.43	0.21	–
N_2	0.29	0.35	0.049	–	0.024	0.043	0.047	0.079	5.9	–	2.5	1.1	3.8	1.1	0.22	0.50	0.12	0.29	0.061	–
CO_2	0.41	0.37	0.029	–	0.037	0.060	0.027	0.063	4.9	–	1.9	1.1	2.6	1.1	0.14	0.47	0.36	0.27	0.21	–

[a]Sources: June et al., 1991; van Krevelen, 1990.

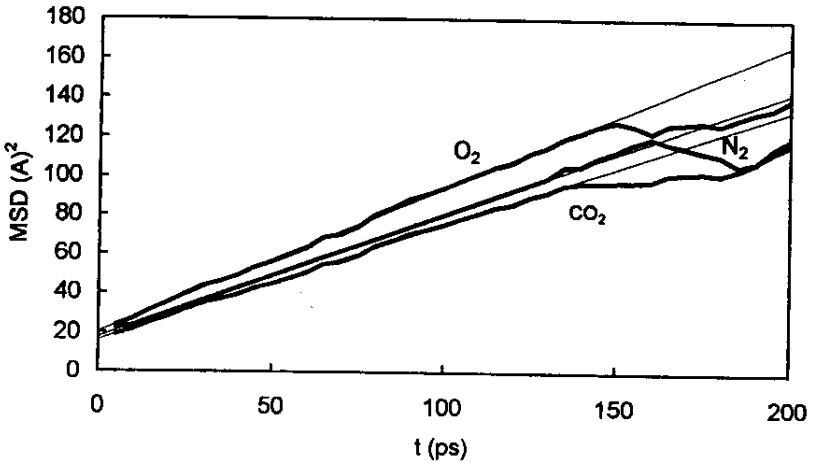

Figure 4. Mean-square displacement (MSD) of O_2, N_2, and CO_2 in *trans* poly(1,4-butadiene) as a function of time. Each thick curve represents the average of the displacements of the five molecules of each gas species, whereas the thin lines are least-square fits to these data.

graphical example of this behavior for *cis* poly(isoprene) and poly(1,2-butadiene), respectively.

The trend revealed by Figures 5 is analogous to that observed, for instance, in MD experiments for the diffusion of the same gases in poly [1-(trimethylsilyl)-1-propyne] (Fried and Goyal, 1998) and in different silicone polymers (Charati and Stern, 1998).

The values of the calculated D of a given gas diffusing in the different rubbery hydrocarbon polymeric matrices also decrease in the following polymer order: *c*-1,4PBD > *t*-1,4PBD > PE > PIB > *c*-PIP > *t*-PIP > *t*-PClP > *c*-PClP > PP > 1,2PBD. The substitution of a bulkier or more rigid functional group such as double bonds or a substituent in a polymeric chain generally limits the intrasegmental mobility of the chain itself,

Table IV Calculated Gas Molecular Volumes

Gas	Volume (Å³)
H_2	12.1
He	10.3
O_2	23.1
N_2	25.2
CO_2	33.1

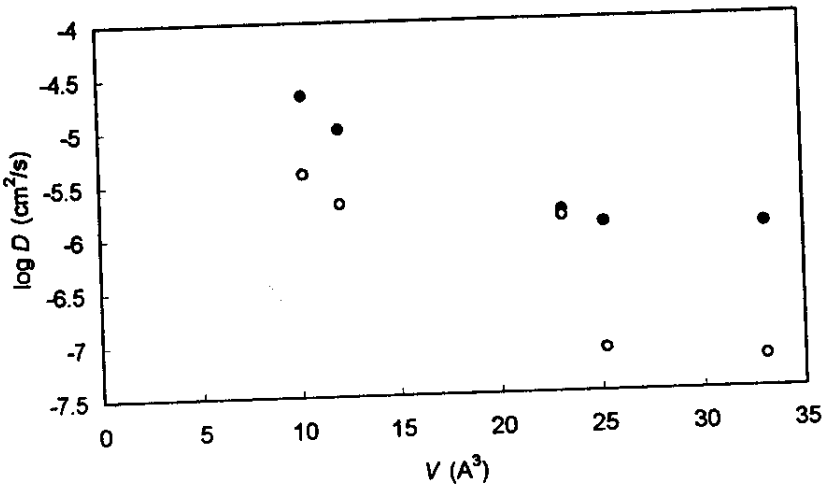

Figure 5. Plot of log D vs. the calculated gas volume for all gases in *cis* poly(1,4-isoprene) (filled symbols) and poly(1,2-butadiene) (open symbols).

which, in turn, is reflected in an increase of the polymer T_g. As a consequence, the diffusivity of gases in the relevant matrices is reduced, since the rate of diffusion of a penetrant molecule depends on the cooperative motion and mobility of the surrounding chains. Accordingly, the results presented in Figure 6, which reports the values of the diffusion coefficient of the various gases in the different matrices as a function of the polymer glass transition temperature, are in harmony with the above observations.

As an example, if we consider poly(ethylene) and poly(propylene), the substitution of a hydrogen in the repeat units with a CH_3 group significantly reduces the mobility of the polymer chains, as indicated by the fact that the T_g of these two hydrocarbon polymers differ by 68 K (see Table I). Accordingly, the values of D of a given gas in these two polymers at the same temperature should be rather different. Table III and Figure 6 show that the values of D obtained from MD simulations for all the gases considered are indeed different, the values for PP being much smaller as expected.

Another interesting consideration concerns the results obtained for stereoisomeric families of polymers. In fact, if we consider Table I again, we can see that, in all cases examined, the *cis* isomers are characterized by lower T_g values with respect to the corresponding *trans* isomers and, hence, we find for these macromolecules higher values of the corresponding experimental diffusion coefficients (compare Table III). And this is exactly what the virtual experiments yield as a result (see again Table III), thus indicating that the models generated and used in our MD

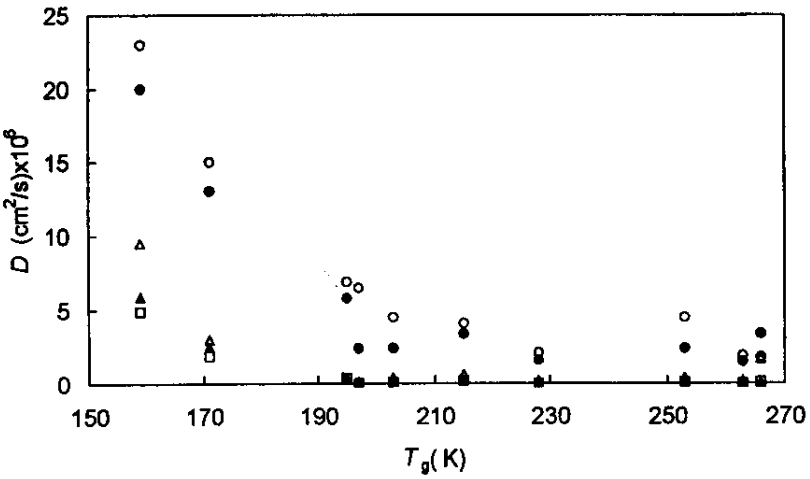

Figure 6. Plot of D vs. the polymer glass transition temperature for all gases. Symbols: open circles, He; filled circles, H_2; open triangles, O_2; filled triangles, N_2; open squares, CO_2.

simulations are able to account even for structural differences such as *cis/trans* geometry, at least within an acceptable degree of accuracy.

Gas Solubility

Fixed-pressure (grand canonical ensemble) sorption computations were carried out for all gases and polymers considered and were used to calculate the solubility coefficients S, as well as the molar heat of solution ΔH_s, as described in the simulation details section. As an example, simulated sorption isotherms for H_2, He, O_2, N_2, and CO_2 in poly(isobutylene) are compared to the relevant experimental values (van Krevelen, 1990) in Figures 7(a) and 7(b), whereas Tables V and VI list all the calculated and the corresponding experimental values (in parenthesis, where available) of the S and ΔH_s, respectively.

Comparison of the sorption isotherms and the values of Tables V and VI show a good agreement between real and virtual experiments for all gases and all polymeric matrices considered. In the case of solubility, the difference between calculated and literature data never exceeds 50%, whereas 1 kJ/mol is the maximum difference found in the comparison of virtual and experimental ΔH_s. The overall good results obtained can be attributed both to the validity of the procedure adopted and to the good parameterization of the LJ and Coulomb parameters of the COMPASS force field. The major differences between virtual and experimental data

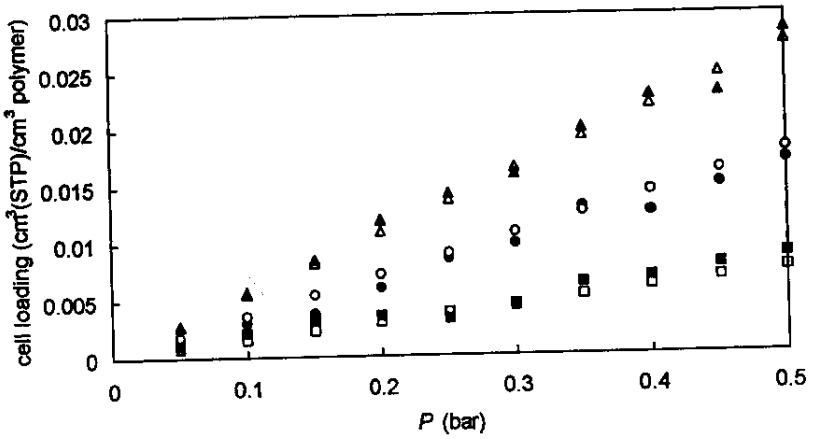

Figure 7(a). Comparison of simulated (filled symbols) and experimental (open symbols) sorption isotherms for He (squares), H_2 (circles), and N_2 (triangles) in poly(isobutylene).

can further be attributed to the fact that, in the simulation technique adopted, the polymeric matrix was treated as a rigid unit, which clearly represents a rough approximation in the case of rubbery amorphous polymers above T_g.

The values reported in Table V deserve a further comment. It is well known experimentally that, for a given gas, the solubilities in the different

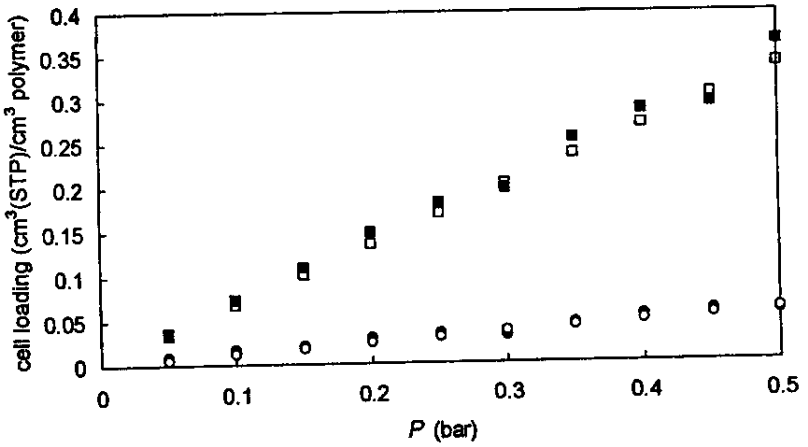

Figure 7(b). Comparison of simulated (filled symbols) and experimental (open symbols) sorption isotherms for O_2 (circles) and CO_2 (squares) in poly(isobutylene).

Table V Comparison Between Experimental and Simulated Solubility Values S (cm^3(STP)/cm^3 bar) at 298 K for All the Gases in All the Polymeric Matrices Considered

GAS	PE		PP		PIB		1,2 PBD		*c*-1,4 PBD		*t*-1,4 PBD		*c*-PIP		*t*-PIP		*c*-PCIP		*t*-PCIP	
	$S_{sim.}$	$S_{exp.}$[a]	$S_{sim.}$	$S_{exp.}$[a]	$S_{sim.}$	$S_{exp.}$[a]	$S_{sim.}$	$S_{exp.}$[a]	$S_{sim.}$	$S_{exp.}$[a]	$S_{sim.}$	$S_{exp.}$[a]	$S_{sim.}$	S_{exp}[a]	$S_{sim.}$	S_{exp}[a]	$S_{sim.}$	S_{exp}[a]	$S_{sim.}$	S_{exp}[a]
H_2	0.042	–	0.024	–	0.025	0.036	0.028	–	0.041	–	0.039	0.033	0.025	0.037	0.028	0.038	0.042	0.026	0.045	–
He	0.035	–	0.013	–	0.021	0.015	0.036	–	0.016	–	0.019	0.015	0.031	0.021	0.030	–	0.0064	0.0071	0.0076	–
O_2	0.046	0.047	0.034	–	0.17	0.12	0.13	–	0.099	–	0.12	0.097	0.28	0.11	0.26	0.10	0.081	0.075	0.073	–
N_2	0.050	0.025	0.033	–	0.057	0.055	0.061	–	0.052	–	0.044	0.045	0.026	0.055	0.032	0.056	0.066	0.036	0.060	–
CO_2	0.39	0.46	0.31	–	0.73	0.68	1.08	–	1.1	–	1.1	1.0	0.92	0.90	1.04	0.97	1.00	0.83	0.95	–

[a]Sources: June et al., 1991; van Krevelen, 1990.

Table VI Comparison Between Experimental and Simulated Heat of Solution ΔH_s (kJ/mol) at 298 K for All the Polymers Considered

GAS	PE		PP		PIB		1,2 PBD		c-1,4 PBD		t-1,4 PBD		c-PIP		t-PIP		c-PCIP		t-PCIP	
	$\Delta H_{s\,sim.}$	$\Delta H_{s\,exp.}$[a]	$\Delta H_{s\,sim.}$	$\Delta H_{s\,exp.}$[a]	$\Delta H_{s\,sim.}$	$\Delta H_{s\,exp.}$[a]	$\Delta H_{s\,sim.}$	$\Delta H_{s\,exp.}$[a]	$\Delta H_{s\,sim.}$	$\Delta H_{s\,exp.}$[a]	$\Delta H_{s\,sim.}$	$\Delta H_{s\,exp.}$[a]	$\Delta H_{s\,sim.}$	$\Delta H_{s\,exp.}$[a]	$\Delta H_{s\,sim.}$	$\Delta H_{s\,exp.}$[a]	$\Delta H_{s\,sim.}$	$\Delta H_{s\,exp.}$[a]	$\Delta H_{s\,sim.}$	$\Delta H_{s\,exp.}$[a]
H_2	2.4	–	2.9	–	2.2	2.5	2.83	–	5.4	–	5.9	6.2	4.1	–	5.6	–	5.9	6.2	4.4	–
He	1.4	–	3.8	–	4.1	–	3.3	–	6.3	–	6.8	7.4	5.0	–	5.3	–	7.5	–	6.2	–
O_2	−2.0	−1.7	−3.3	–	−4.7	−5.0	−4.7	–	1.2	–	0.99	1.3	−5.0	−4.2	−6.2	–	2.0	2.3	1.4	–
N_2	2.5	2.1	2.2	–	1.9	1.7	1.7	–	4.3	–	3.8	4.2	3.5	2.1	2.3	–	1.4	–	0.93	–
CO_2	−6.0	−5.3	−10.1	–	−9.2	−8.8	−12.0	–	−7.6	–	−7.9	−8.8	−12.8	−12.5	−13.5	–	−10.6	−9.6	−12.0	–

[a]Sources: June et al., 1991; van Krevelen, 1990.

polymers do not show large variations. The nature of the gas, however, is important. As we can see from Table V, the results obtained from simulation reflect this trend, the exceptions being due to larger deviations from the experimental values. The same comments apply to the values of the molar heat of solution. For the smallest gas molecules (i.e., H_2 and He) dissolving in rubbery amorphous polymers, the simulation predicts an endothermic effect, being ΔH_s positive; for the larger gases, the reverse is true and, according to the experimental evidence, the simulation yields negative values of ΔH_s. This implies that, in the case of an exothermic effect, the sorption energy evolved exceeds the energy needed to make a hole of molecular size in the polymer. Further, as for the solubility values, the ΔH_s values of rubbery polymers also mainly depend on the nature of the gases and not on the nature of the polymer matrix. This is correctly predicted from simulation, as reported in Table VI.

CONCLUSIONS

In this paper we have presented the results obtained from atomistic virtual experiments of both diffusion and absorption phenomena of different gases in several amorphous rubbery polymeric matrices. Excellent agreement was found between the experimental diffusion coefficients D for H_2, He, O_2, N_2, and CO_2 and the corresponding values obtained using molecular dynamics simulations. Further, good simulated sorption isotherms were obtained in all cases by the application of the fixed pressure grand canonical Monte Carlo technique; from these data, the corresponding values of the gas solubility S and the molar heat of solution ΔH_s were obtained and compared with the relevant experimental information. The good agreement of the virtual and experimental data sets can be attributed to the validity of the intermolecular potential selected, whereas the major discrepancies can be ascribed to the rigidity imposed onto the polymeric matrix by the GCMC technique.

According to the results obtained, we can conclude that both the MD and GCMC techniques adopted in this work can be considered reliable tools to predict, with an acceptable degree of accuracy, the diffusion and solubility of gases into amorphous rubbery polymeric matrices, and further work is currently in progress to test these methods for the determination of the temperature dependence of these phenomena.

ACKNOWLEDGMENT

The authors wish to thank the Italian Ministry for University and Scientific Research (MURST, Roma, Prin 99) and the University of Trieste (Special Grant for Scientific Research) for financial support.

APPENDIX

The total potential energy E_p of the COMPASS force field is expressed as a combination of valence terms, including diagonal and off-diagonal cross-coupling terms, and nonbonded interaction terms. The analytical form of E_p can then be written as:

$$
\begin{aligned}
E_p = & \sum_b \left[K_2(b-b_0)^2 + K_3(b-b_0)^3 + K_4(b-b_0)^4\right] \\
& + \sum_\theta \left[H_2(\theta-\theta_0)^2 + H_3(\theta-\theta_0)^3 + H_4(\theta-\theta_0)^4\right] \\
& + \sum_\phi \left\{V_1\left[1-\cos\left(\phi-\phi_1^0\right)\right] + V_2\left[1-\cos\left(2\phi-\phi_2^0\right)\right]\right. \\
& \left. + V_3\left[1-\cos\left(3\phi-\phi_3^0\right)\right]\right\} \\
& + \sum_\chi K_\chi \chi^2 \sum_b \sum_{b'} F_{bb'}(b-b_0)\left(b'-b_0'\right) \\
& + \sum_\theta \sum_{\theta'} F_{\theta\theta'}(\theta-\theta_0)\left(\theta'-\theta_0'\right) \\
& + \sum_b \sum_\theta F_{b\theta}(b-b_0)(\theta-\theta_0) \\
& + \sum_b \sum_\phi (b-b_0)(V_1\cos\phi + V_2\cos 2\phi + V_3\cos 3\phi) \\
& + \sum_{b'} \sum_\phi \left(b'-b_0'\right)(V_1\cos\phi + V_2\cos 2\phi + V_3\cos 3\phi) \\
& \times \sum_\theta \sum_\phi (\theta-\theta_0)(V_1\cos\phi + V_2\cos 2\phi + V_3\cos 3\phi) \\
& + \sum_\phi \sum_\theta \sum_{\theta'} K_{\phi\theta\theta'}\cos\phi(\theta-\theta_0)\left(\theta'-\theta_0'\right) \\
& + \sum_{i>j} \frac{q_i q_j}{r_{ij}} + \sum_{i>j} E_{ij}\left[2\left(\frac{r_{ij}^0}{r_{ij}}\right)^9 - 3\left(\frac{r_{ij}^0}{r_{ij}}\right)^6\right]
\end{aligned}
$$

REFERENCES

Allen, M. P. and Tildesley, D. J. (1987). *Computer Simulation of Liquids*, Clarendon Press, Oxford, U.K.

Andersen, H. C. (1980). *J. Chem. Phys.*, **72**, 2384.

Berendsen, H. J. C., Postma, J. P. M., van Gunsteren, W. F., DiNola, A. and Haak, J. R. (1984). *J. Chem Phys.*, **81**, 3684.

Brooks, C. L., Montgomery, R., Pettitt, B. and Karplus, M. (1985). *J. Chem. Phys.*, **83**, 5897.

Ceperley, D., ed. (1980). *The Problem of Long-range Forces in the Computer Simulation of Condensed Media*, National Information Information Service, Springfield, Varginia.

Charati, S. G. and Stern, S. A. (1998). *Macromolecules*, **31**, 5529.

Connolly, M. L. (1983a). *J. Appl. Crystallogr.*, **16**, 548.

Connolly, M. L. (1983b) *Science*, **221**, 709.

Connolly, M. L. (1985). *J. Am. Chem. Soc.*, **107**, 1118.

Crank, J. (1975). *The Mathematics of Diffusion*, 2nd ed., Clarendon Press, Oxford, U.K.

Crank, J. and Park, G. S. eds. (1968). *Diffusion in Polymers*, Academic Press, New York.

Fan, C. F., Cagin, T., Chen, Z. M. and Smith, K. A. (1994). *Macromolecules*, **27**, 2383.

Fermeglia, M. and Pricl, S. (1999). *Fluid Phase Equil.*, **166**, 21.

Flory, P. J. (1974). *Principles of Polymer Chemistry*, Cornell University Press, Ithaca, NY.

Fried, J. R. and Goyal, D. K. (1998). *J. Polym. Sci. Part B: Polym Phys.*, **36**, 519.

Gusev, A. A., Müller-Plathe, F., van Gunsteren, W.F. and Suter, U. (1994). *Adv. Polym. Sci.*, **116**, 207.

Hildebrand, J. H. and Scott, R. (1949). *Solubility of Non-electrolytes*, 3rd ed., Reinhold, New York.

June, R. L., Bell, A. T. and Theodorou, D. N. (1991). *J. Phys. Chem.*, **95**, 8866.

Koros, W. J. and Paul, D. R. (1978). *J. Polym. Sci. Polym. Phys. Ed.*, **16**, 1947.

Khrisna Pant, P. V. and Boyd, R. H. (1993). *Macromolecules*, **26**, 679.

Kulkarni, S. S. and Stern, S. A. (1983). *J. Polym. Sci. Polym. Phys. Ed.*, **21**, 441.

Li, Y. and Mattice, W. L. (1992). *Macromolecules*, **25**, 4942.

Maple, J. R., Dinur, U. and Hagler, A. T. (1988). *Proc. Natl. Acad. Sci.*, **85**, 5350.

Mark, J. H. (1997). *Handbook of Polymer Properties*, American Physical Society, New York.

Mattice, W. L. and Suter, U.W. (1994). *Conformational Theory of Large Molecules: The Rotational Isomeric State Model in Macromolecular Systems*, John Wiley, New York.

Petropoulos, J. H. (1970). *J. Polym. Sci. Polym. Phys. Ed.*, **8**, 1979.

Rappé, A. K. and Goddard III, W. A. (1991). *J. Phys. Chem.*, **95**, 3358.

Rellick, L. M. and Becktel, W. J. (1997). *Biopolymers*, **42** 191.

Rodgers, P. A. (1993). *J. Appl. Polym. Sci.*, **48**,1061.

Sonnenburg, J., Gao, J. and Weiner, J. H. (1990). *Macromolecules*, **23**, 4653.

Stern, S. A. and Trohalaki, B. (1990). In *Barrier Polymers and Structure*, ed. W. J. Koros, ACS Symposium Series 423, American Chemical Society, Washington, D.C., 22–70.

Stern, S. A., Sampat, S. R. and Kulkarni, S. R. (1986). *J. Polym. Sci. Polym. Phys. Ed.*, **24**, 2149.

Sun, H. (1998). *J. Phys. Chem.*, **102**, 7338.
Sun, H. and Rigby, D. (1997). *Spectrochimica Acta* (*A*), **53**, 1301.
Takeuchi, H. and Okazaki, K. (1990). *J. Chem. Phys.*, **92**, 5643.
Theodorou, D. N. (1996). In *Diffusion in Polymers*, ed. P. Neogi, Marcel Dekker, New York, 67.
Theodorou, D. N. and Suter, U. W. (1985). *Macromolecules*, **18**, 1467.
van der Vegt, N. F. A., Briels, W. J., Wessling, M. and Strathmann, H. (1998). *J. Chem. Phys.*, **108**, 9558.
van Krevelen, D. W. (1990). *Properties of Polymers: Their Correlation with Chemical Structure, Their Numerical Estimation and Prediction from Additive Group Contributions*. Elsevier Science, Amsterdam.
Verlet, L. (1967). *Phys. Rev.*, **159**, 98.
Waldman, M. and Hagler, A. T. (1993). *J. Comput. Chem.*, **14**, 1077.
Zhou, S. and Stern, S. A. (1989). *J. Polym. Sci. Polym. Phys. Ed.*, **27**, 205.